# Circulating miRNAs as potentially predictive biomarkers for chemoimmunotherapy in advanced biliary tract cancer: a post-hoc analysis of the phase II T1219 study

Check for updates

Nai-Jung Chiang[1,2,3], Cheng-Yu Tang[1,2,4], Li-Yuan Bai[5], Po-Chang Chang[6], Wei-Ming Chen[6], Shih-Ting Kang[6], San-Chi Chen[1,2], Ming-Huang Chen[1,2,10] & Jason Chia-Hsun Hsieh [7,8,9,10] ✉

Circulating microRNAs (miRNAs) have not been investigated as predictive biomarkers in patients with advanced biliary tract cancer (ABTC) who received chemoimmunotherapy. In the single-arm phase II T1219 trial, 46 patients with ABTC received first-line nivolumab, gemcitabine, and S-1 treatment. Plasma samples were prospectively collected at baseline and 6 weeks after treatment for miRNA profiling. Among the 167 miRNAs analyzed, the baseline levels of hsa-miR-16-5p, hsa-miR-93-5p, and hsa-miR-126-3p were significantly elevated in the responders. High hsa-miR-16-5p expression was correlated with longer progression-free survival (hazard ratio [HR] = 0.44, 95% confidence interval [CI] = 0.12–0.85, $p$ = 0.025) and overall survival (HR = 0.34, 95% CI = 0.07–0.7, $p$ = 0.01). Post-treatment miRNA changes (e.g., hsa-miR-129-5p and hsa-miR-1254) were observed but were not significantly associated with survival. This study identified a three-miRNA signature with potential predictive value for chemoimmunotherapy in ABTC. Trial registration: NCT04172402, date of registration 2019/11/18.

Biliary tract cancer (BTC) is a heterogeneous group of malignancies that includes intrahepatic cholangiocarcinoma, extrahepatic cholangiocarcinoma, and gallbladder cancer. Although surgical resection is the only curative option, disease recurrence is common and often difficult to manage with local therapies, underscoring the critical need for effective systemic treatments[1]. Currently, the first-line treatment for advanced BTC includes gemcitabine and cisplatin in combination with immune checkpoint inhibitors (ICIs), such as programmed death 1 (PD-1) or programmed death-ligand 1 (PD-L1) inhibitors, which have demonstrated survival benefits over chemotherapy alone in large phase III trials[2,3].

These advances have redefined the treatment paradigm; however, identifying robust predictive biomarkers of chemoimmunotherapy response in BTC remains a challenge. Microsatellite instability-high (MSI-H), a well-known biomarker for immunotherapy efficacy, is rarely observed in BTC[4–6], limiting its clinical relevance. Although PD-L1 expression is widely used in other cancer types, it has shown inconsistent predictive values in BTC because of the heterogeneity in detection antibodies, scoring systems, and cutoff thresholds[2,3]. Thus, there is a need to discover potential noninvasive biomarkers to guide patient selection for immunotherapy-based treatments.

[1]Department of Oncology, Taipei Veterans General Hospital, Taipei, Taiwan. [2]School of Medicine, College of Medicine, National Yang Ming Chiao Tung University, Taipei, Taiwan. [3]National Institute of Cancer Research, National Health Research Institutes, Tainan, Taiwan. [4]Institute of Clinical Medicine, National Yang Ming Chiao Tung University, Taipei, Taiwan. [5]Division of Hematology and Oncology, Department of Internal Medicine, China Medical University Hospital and China Medical University, Taichung, Taiwan. [6]Quark Biotechnology Inc., Hsinchu, Taiwan. [7]Division of Hematology-Oncology, Department of Internal Medicine, Chang Gung Memorial Hospital at Linkou, Taoyuan City, Taiwan. [8]College of Medicine, Chang Gung University, Taoyuan City, Taiwan. [9]School of Medicine, National Tsing Hua University, Hsinchu City, Taiwan. [10]These authors contributed equally: Ming-Huang Chen, Jason Chia-Hsun Hsieh. ✉e-mail: wisdom5000@gmail.com

THE HORMEL INSTITUTE
UNIVERSITY OF MINNESOTA

Among blood-based biomarkers, carbohydrate antigen 19-9 (CA19-9) is the most commonly used biomarker for BTC. However, its utility is primarily prognostic rather than predictive, and its expression is absent in some patients owing to fucosyltransferase deficiency[7]. In recent years, circulating biomarkers, including cell-free DNA, circulating tumor cells, and extracellular vesicle-associated molecules, have garnered attention in oncology. Circulating tumor DNA (ctDNA) has shown promise for mutation profiling and minimal residual disease detection in BTC; however, its predictive role in immunotherapy remains exploratory[8]. This highlights the need for novel circulating biomarkers that are both mechanistically informative and clinically relevant to the disease.

MicroRNAs (miRNAs) are small non-coding RNAs that regulate gene expression through mRNA degradation or translational repression. Dysregulation has been implicated in numerous cancer-related pathways, including proliferation, apoptosis, angiogenesis, and metastasis[9]. Aberrant miRNA expression may serve as a predictive biomarker for BTC. Multiple studies have reported that aberrant miRNA expression profiles are associated with prognosis and treatment response in BTC[10–12]. Several miRNA panels have been proposed as diagnostic or prognostic classifiers, and specific miRNAs have been linked to chemotherapy sensitivity or resistance[13,14]. Emerging evidence suggests that miRNAs may modulate immune-related pathways, including antigen presentation and interferon-γ signaling, potentially influencing the response to ICIs[15]. However, most previous studies were conducted in patients with ICI-naïve diseases and focused on diagnosis or prognosis, leaving the predictive role of miRNAs in the context of chemoimmunotherapy largely unexplored.

Recent studies on hepatocellular carcinoma and lung cancer have demonstrated that panels of circulating miRNAs outperform single biomarkers in predicting treatment response[16,17]. This likely reflects the complex and multifactorial nature of tumor-immune interactions, as individual miRNAs often regulate distinct yet partially overlapping oncogenic and immunologic pathways. Thus, a combined miRNA signature, referring to a specific pattern or profile of miRNA expression levels, may better capture the underlying biological complexity associated with the response to chemoimmunotherapy.

Based on this rationale, we conducted a prospective biomarker analysis using peripheral blood samples collected during the phase II T1219 study, which evaluated nivolumab in combination with gemcitabine and S-1 in patients with advanced BTC[18]. In this post-hoc analysis (as shown in Fig. 1), we aimed to identify circulating miRNAs with potential predictive values for treatment response, using a machine learning (ML)-based approach to integrate multifactorial signals and inform personalized therapeutic strategies in this challenging disease setting.
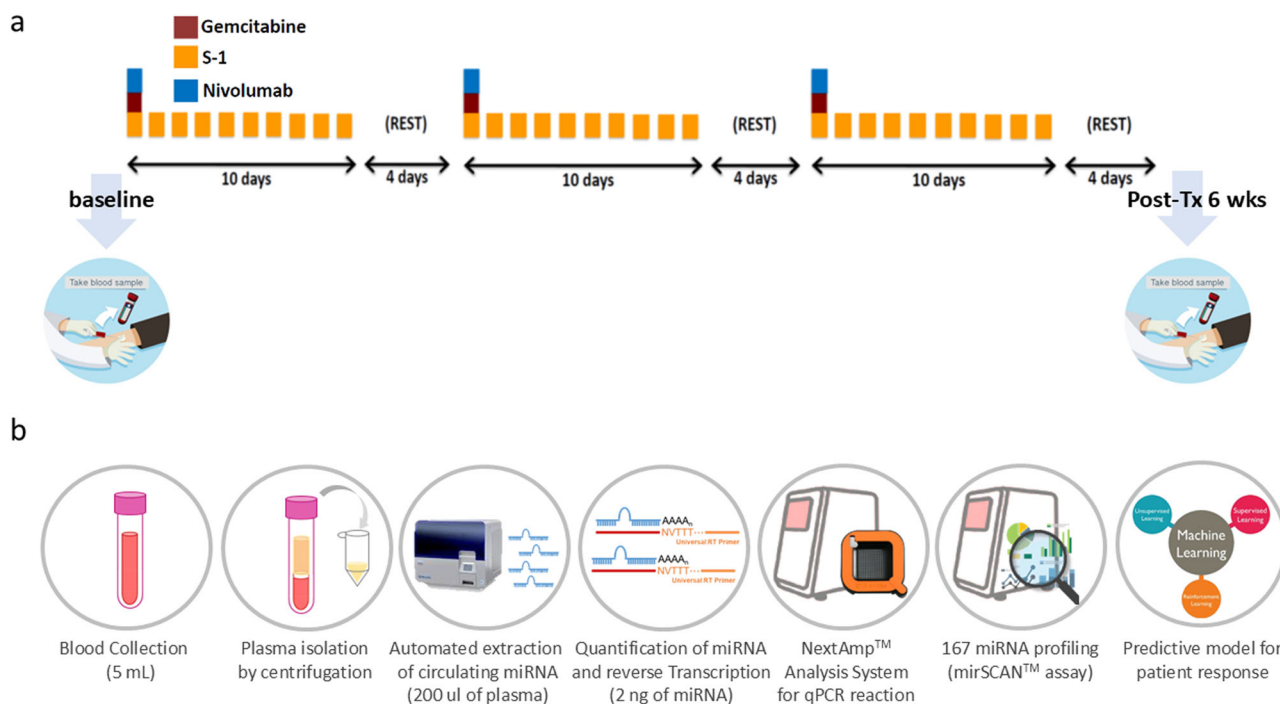
## Results

### Clinical patient characteristics

In total, 48 patients were enrolled in the T1219 trial, and their characteristics are summarized in Table 1. Two patients were excluded from the analyses: one because of loss to follow-up and the other because of hemolysis of plasma samples. Consequently, 46 patients were included in the final analysis. Based on the best tumor response during treatment, patients were classified as responders (CR, complete response or PR, partial response) or non-responders (SD, stable disease or PD, progression disease). Accordingly, 21 patients were classified as responders, including one with CR and 20 with PR, while 25 patients were non-responders, including 20 with SD and five with PD-L1 expression and tumor mutational burden (TMB) status were previously assessed in the original T1219 study cohort, with 41% of patients exhibiting PD-L1 positivity and 15% classified as TMB-high (TMB-H), based on a BTC-specific cutoff of 7.1 mutations/Mb, as reported in our prior publication. Only one patient had a tumor with MSI-H status.

Seven additional patients with advanced BTC were recruited from other sites for the independent validation of the model. Most patients were female (71.4%) and had stage-IV disease (85.7%). All patients received anti-PD-1 therapy, including pembrolizumab (n = 6) or nivolumab (n = 1). Two patients were classified as responders and five as non-responders (Table S2).

### Building an miRNA-based model for predicting treatment response

We evaluated the correlation between baseline circulating miRNAs and response to chemoimmunotherapy using a 167-miRNA panel. Subsequently, 39 miRNAs expressed in more than 80% of the samples from both



**Fig. 1 | Overview of the correlation analyses of miRNAs in the T1219 study. a** The T1219 study was a single-arm phase II trial to administer biweekly nivolumab in combination with gemcitabine and S-1 as the first-line treatment in advanced BTC. The parallel plasma samples of pre- and post-treatment after 6 weeks were collected from 46 patients. **b** Plasma samples were subjected to circulating miRNA extraction, reverse transcription, and miRNA profile analyses.

**Table 1 | Baseline demographics and clinical characteristics**

| | Patients (N = 46) |
|---|---|
| **Age (yrs)** | |
| Median (range) | 67 (30–80) |
| < 65 | 18 (39.1) |
| ≥ 65 | 28 (60.9) |
| **Sex** | |
| Male | 20 (43.4) |
| Female | 26 (56.5) |
| **Primary site** | |
| Intrahepatic | 28 (60.9) |
| Extrahepatic | 11 (23.9) |
| Gallbladder | 5 (10.9) |
| Ampulla vater | 2 (4.3) |
| **Disease status** | |
| Locally advanced | 6 (13) |
| Distant Metastasis | 40 (87) |
| **Chronic hepatitis** | |
| HBV | 12 (26) |
| HCV | 2 (4) |
| **Treatment response** | |
| Responders | 21 (45.6) |
| Non-responders | 25 (54.3) |
| **PD-L1 expression** | |
| CPS ≥ 1 | 19 (41.3) |
| CPS ≥ 10 | 13 (28.3) |
| Not assessable | 1 (2.2) |
| **TMB** | |
| TMB-H (≥ 7.1 mut/Mb) | 7 (15.2) |
| TMB-L (< 7.1 mut/Mb) | 25 (54.3) |
| Not assessable | 14 (30.4) |

*PD-L1* programmed death-ligand 1, *CPS* combined positive score, *TMB* tumo mutation burden, *TMB-H* tumor mutation burden high, *TMB-L* tumor mutation burden low.

responders and non-responders were selected to develop an miRNA-based classifier according to tumor response (Table S1). Using a 10-fold cross-validation approach, we developed an miRNA-based classifier and fine-tuned its parameters to achieve better performance. The sensitivity and specificity of this classifier were 76.19 and 68.00% for the training set (T1219 cohort) and 50.00 and 80.00% for the testing set (an independent cohort), respectively. The accuracies were 71.74 and 71.43% for the training and testing sets, respectively (Table S3).

### Baseline circulating miRNAs associated with response to chemoimmunotherapy

Among the 39 circulating miRNAs evaluated, we identified hsa-miR-16-5p, hsa-miR-93-5p, and hsa-miR-126-3p as the top three candidates for inclusion in the miRNA-based classifier. These miRNAs were significantly upregulated in responders compared to non-responders (Fig. 2A), met the criterion of being detectable in more than 80% of the 46 cases, and showed statistically significant differences in Cq values between groups (Student's t-test, $p < 0.05$). A summary of the statistical results for all 39 miRNAs is provided in Table S1. We further evaluated the correlation between these differentially expressed miRNAs and the therapeutic response using receiver operating characteristic (ROC) curve analysis (Fig. 2B). The combination of these three miRNAs demonstrated the best predictive value (area under the curve (AUC) = 0.81) compared

to that of the individual miRNAs ($p < 0.05$, multivariate analysis of variance (MANOVA)).

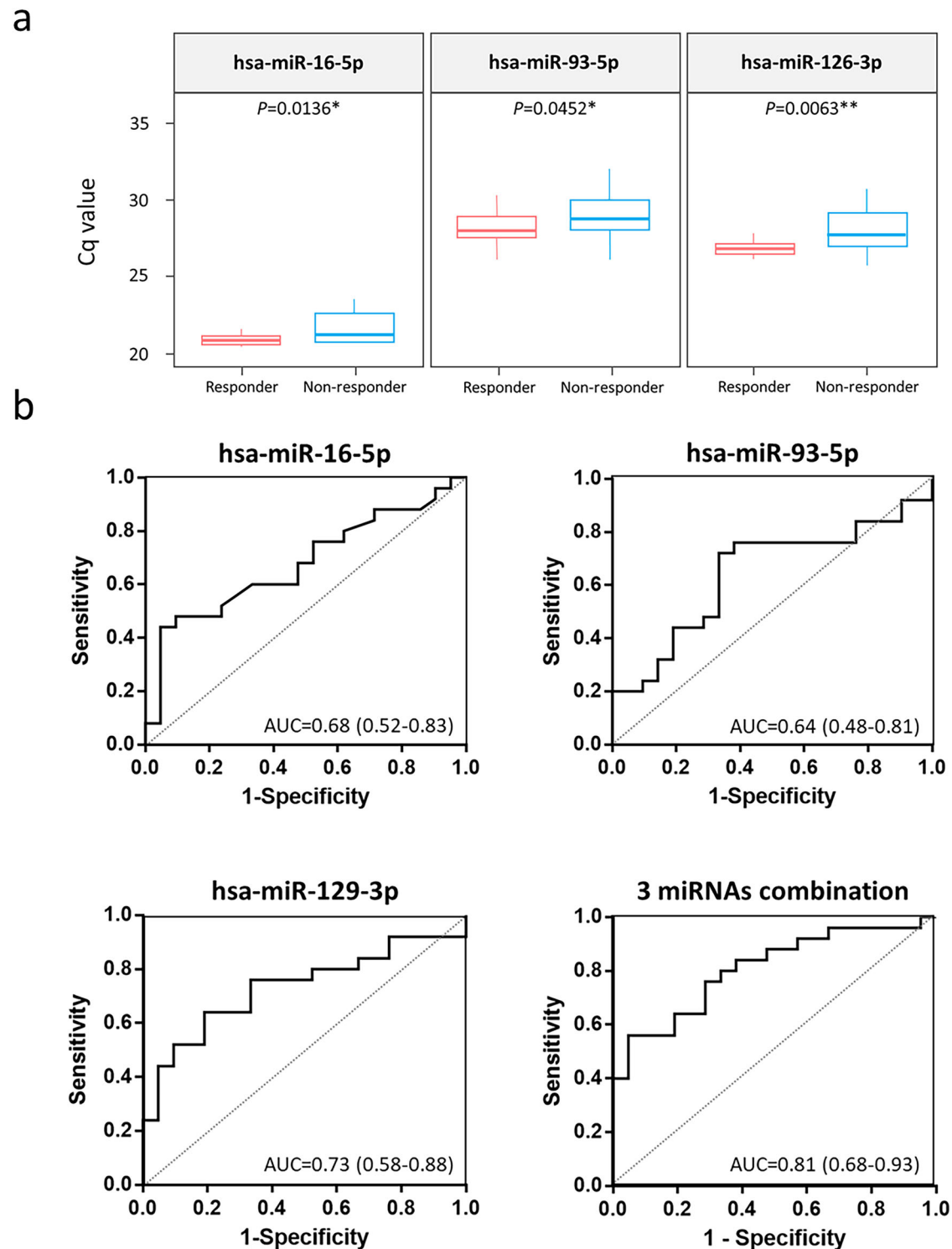### Differentially expressed miRNAs associated with survival

We assessed patient outcomes based on the expression levels of three miRNAs (hsa-miR-16-5p, hsa-miR-93-5p, and hsa-miR-126-3p). Progression-free survival (PFS) was significantly better in the group with high expression of hsa-miR-16-5p and hsa-miR-93-5p than in those with low expression ($p = 0.025$ and 0.036, HR [95% CI, confidence interval] = 0.44 [0.12–0.85] and 0.59 [0.28–1.07], respectively) (Fig. 3A). High expression of hsa-miR-16-5p, hsa-miR-126-3p, and a combination of these three miRNAs correlated with longer overall survival (OS) ($p = 0.01$, 0.001, and 0.013, HR [95% CI] = 0.34 [0.07–0.7], 0.28 [0.09–0.55], and 0.38 [0.12–0.77], respectively) (Fig. 3B). Among these three miRNAs, only hsa-miR-16-5p expression was associated with both PFS and OS. We further examined the relationship between these miRNAs and the regulatory frameworks of the PD-1/PD-L1 checkpoint and interleukin (IL) signaling. This was achieved through functional enrichment analysis using STRING-DB v11.5, and the results were visualized using Cytoscape 3.9 (Fig. 3C). The top three hub genes identified were *TP53*, *AKT1*, and *MTOR*, indicating that miRNAs may interact with *TP53*, *AKT1*, and *MTOR* to influence the chemoimmunotherapy response and patient outcomes.

### The correlation between miRNA and PD-L1 expression, tumor mutation burden

The patients were divided into two groups based on the PD-L1 combined positive score (CPS), defined as the ratio of PD-L1-stained tumor and immune cells to all viable tumor cells. The expression of hsa-miR-19a-3p and hsa-miR-16-5p was significantly different between PD-L1 ≤ 1 and PD-L1 ≥ 10, with *p-values* of 0.0086 and 0.028, respectively (Fig. S1A). The predictive power of miRNAs for PD-L1 expression was evaluated using ROC curve analysis, with AUC values of 72% for hsa-miR-19a-3p and 58% for hsa-miR-16-5p. However, combining these two miRNAs did not improve predictive power (Fig. S1B). We further analyzed the interactions of hsa-miR-19a-3p and hsa-miR-16-5p with PD-1/PD-L1 and IL signaling (Fig. S1C). The top five hub genes were *PTEN*, *MTOR*, *KRAS*, *PIK3CA*, and *CHUK*. We also assessed the correlation between miRNAs and TMB. Although no significant association was found, TMB may be a useful biomarker for predicting chemoimmunotherapy outcomes in patients with advanced BTC. We combined TMB with the baseline expression levels of three miRNAs (hsa-miR-16-5p, hsa-miR-93-5p, and hsa-miR-126-3p) to construct a prediction model for PFS, which demonstrated an improved predictive value (AUC = 0.92) compared to that of the individual markers (Fig. S2a, b). In comparison, PD-L1 expression alone yielded lower predictive accuracy, with AUCs of 0.55 for PFS and 0.65 for OS (Fig. S2c, d). These findings suggest that the integrated miRNA + TMB model provides improved prognostic stratification compared to PD-L1 alone.

### The dynamic change in miRNA correlated with treatment response and survival

Parallel plasma samples collected before and after 6 weeks of treatment from all 46 patients were analyzed in this study. After treatment, four miRNAs were differentially expressed compared to baseline levels (fold change > ±2 and $p < 0.05$), including downregulation of hsa-miR-129-5p in the PD group, upregulation of hsa-miR-1254 and hsa-miR-574-3p in the responders, and downregulation of hsa-miR-1290 in the responders (Table 2 and Fig. S3). We further evaluated the correlation between dynamic changes in miRNA levels and therapeutic outcomes (PFS and OS). Only hsa-miR-129-5p showed borderline significance ($p = 0.07$, HR [95% CI] = 2.084 [0.94–5.53]) for OS (Fig. 4A). Pathway analysis indicated that hsa-miR-129-5p is involved in several important signaling pathways, such as PI3K-AKT, the immune system, and Toll-like receptor signaling pathways (Fig. 4B), suggesting a possible tumor-suppressive role for hsa-miR-129-5p in advanced BTC.

a



b



**Fig. 2 | Differentially expressed miRNAs were identified between responders and non-responders (fold change > ± 1.5 and *p* value < 0.05). a** Three miRNAs were differentially expressed in advanced BTC. hsa-miR-16-5p, hsa-miR-93-5p, and hsa-miR-126-3p were up-regulated significantly in responders. The predictive value of the miRNA-based therapeutic response classifier was analyzed using the ROC curve. **b** Prediction model combining all three miRNAs using logistic Lasso regression showed the best AUC value at 0.81 compared to the models built on each individual miRNA. 95% confidence intervals are shown in parentheses.

## Discussion

Chemoimmunotherapy is currently the standard first-line treatment for advanced BTC; however, no reliable biomarkers have been established to predict the treatment response, PFS, or OS. Although PD-L1 expression has been explored in previous studies, including two phase III trials (TOPAZ-1 and KEYNOTE-966) and our own phase II T1219 trial, its predictive value remains inconsistent in combination therapy settings. Other tissue-based biomarkers, such as TMB, MSI, and DNA damage repair alterations, have shown limited applicability and often require invasive sampling, which is not feasible in many patients[4,19–21]. Circulating biomarkers have emerged as promising alternatives to address these limitations, with miRNAs and ctDNAs being among the most widely studied. Compared to ctDNA, miRNAs may offer enhanced biological insights into tumor-immune system interactions and are particularly suited for longitudinal monitoring[22–24].
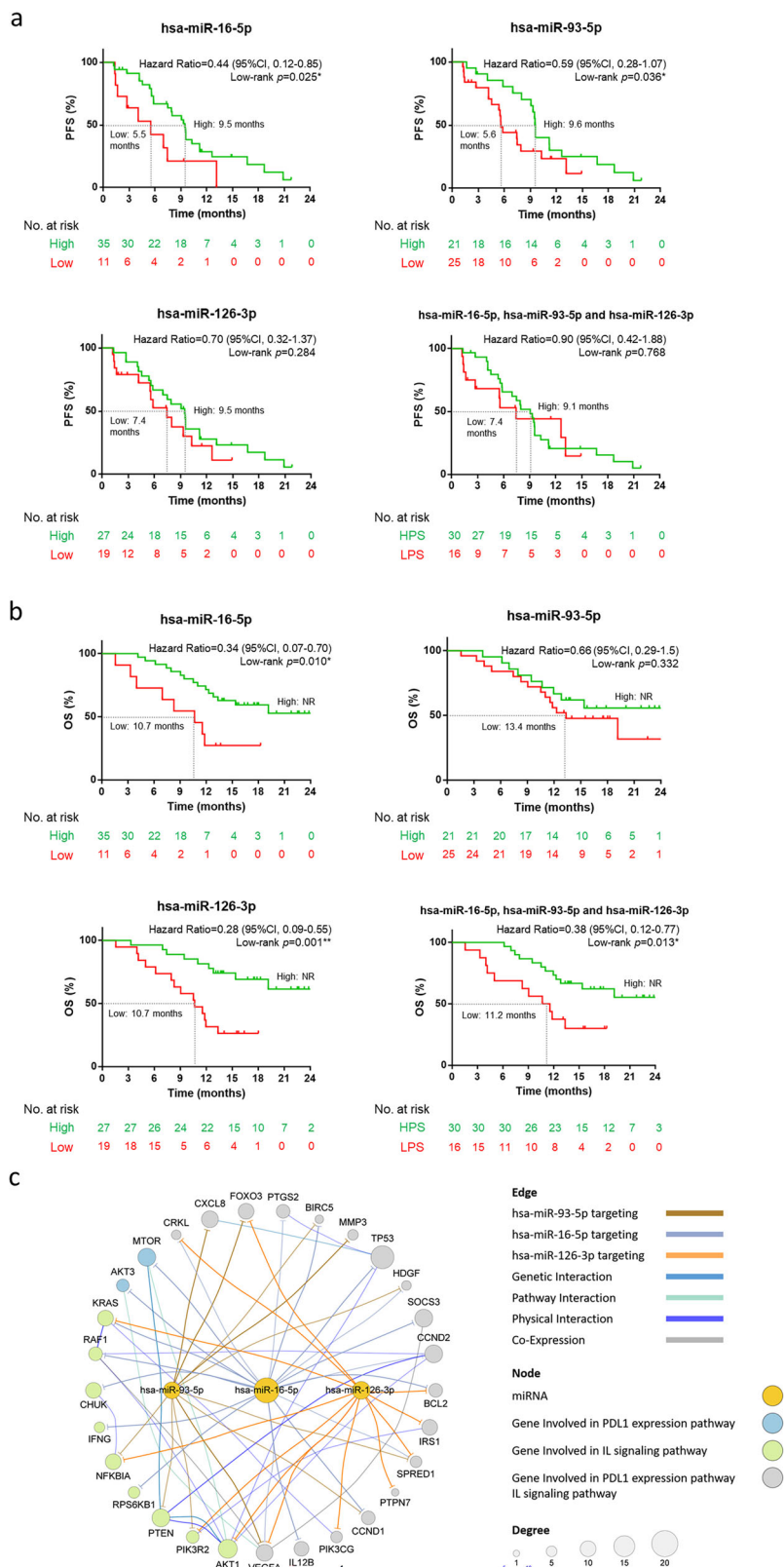
**Fig. 3 | Survival analysis and potential regulatory mechanism of differentially expressed miRNAs.** **a** High expression of hsa-miR-16-5p and hsa-miR-93-5p significantly correlated with a longer PFS. **b** hsa-miR-16-5p, hsa-miR-126-3p, and the combination of the three miRNAs associated with a significant overall survival difference. The combination prediction score was derived from logistic Lasso regression using the three miRNAs, dividing patients into two groups: high prediction score (HPS) and low prediction score (LPS). **c** An interaction network of miRNA target genes involved in IL-signaling and PD-1/PD-L1 pathway was analyzed using STRING-DB and Cytoscape. Edge color represented different interaction type whereas edge width represented the interaction evidence level. The node size accounted for the edges connected to the node. The top 3 hub genes were TP53, AKT1, and *MTOR*, which showed the highest degree score analyzed by Cytoscape.



In this prospective biomarker study embedded within the phase II T1219 trial, we employed a BTC-focused plasma miRNA panel to identify three miRNA signatures—hsa-miR-16-5p, hsa-miR-93-5p, and hsa-miR-126-3p —associated with treatment response and survival outcomes in patients receiving nivolumab, gemcitabine, and S-1. The potential predictive value of this signature was validated in an independent patient cohort. These findings not only highlight the potential of miRNAs as accessible and informative biomarkers for immunotherapy but also align with prior observations in melanoma, further supporting their broader relevance in cancer immunotherapy[25].

The roles of miRNAs in the oncogenesis, diagnosis, and prognosis of BTC have been studied for several decades now. Several miRNAs, including

**Table 2 | The dynamic change in miRNAs was identified based on two-time fold change and *p* value < 0.05 by *t* test**

| miRNA | Fold change (post/pre) | *p* value (*t* test) |
|---|---|---|
| **Progression disease (N = 5)** | | |
| hsa-miR-129-5p | −2.36 | 0.03507[a] |
| **Partial response/complete response (N = 21)** | | |
| hsa-miR-1254 | 2.45 | 0.00958[a] |
| hsa-miR-1290 | −2.79 | 0.04016[a] |
| hsa-miR-574-3p | 2.22 | 0.01886[a] |

[a] indicated statistical significance.

hsa-miR-21, hsa-miR-221, hsa-miR-26a, hsa-miR-192, hsa-miR-29a, hsa-miR-151-3p, hsa-miR-126, hsa-miR-106a, hsa-miR-146a, hsa-miR-31, hsa-miR-203, hsa-miR-191, and hsa-miR-195 are considered prognostic markers[26]. These miRNAs were included in our study panel; however, only hsa-miR-126 showed prognostic significance. hsa-miR-126 is a tumor suppressor that negatively regulates the expression of vascular endothelial growth factor (VEGF) and solute transporter family 7 member 5[27,28]. hsa-miR-126 is commonly downregulated in certain cancer types, including lung, pancreatic, esophageal, hepatocellular carcinoma, and BTC[29]. Restoration of hsa-miR-126 expression suppresses VEGF expression and inhibits the growth of lung cancer cell lines[28]. Low hsa-miR-126 expression is considered a negative prognostic factor associated with shorter PFS and OS in lung cancer[30]. In our study, advanced BTC with low hsa-miR-126 expression was correlated with unfavorable OS compared to those with high expression (10.7 months versus not reached). However, low hsa-miR-126 expression was a good prognostic indicator in McNally's study, which examined tumor tissue samples from patients with surgically resected BTC[31]. Differences in tumor characteristics and treatments may contribute to the varying findings regarding the influence of hsa-miR-126 on BTC. Further studies are necessary to determine the prognostic value of hsa-miR-126 in BTC.

In our analyses, hsa-miR-16-5p and hsa-miR-93-5p also exhibited prognostic value in advanced BTC. hsa-miR-16 acts as a tumor suppressor and potentially downregulates Yes-associated protein 1 (YAP-1). Plasma hsa-miR-16 levels have been tested as diagnostic biomarkers for differentiating distal cholangiocarcinoma from normal tissue or pancreatic duct adenocarcinoma[32,33]. In contrast, hsa-miR-93 promotes tumor growth and cancer progression and is significantly upregulated in many cancer types, including hepatocellular carcinoma, pancreatic cancer, gastric cancer, and bladder cancer[34–37]. However, neither hsa-miR-16 nor hsa-miR-93 has been previously reported to have prognostic significance in BTC, as shown in this study.

The interaction between miRNAs and the PD-1/PD-L1 pathway is well established, with several miRNAs directly modulating PD-L1 expression or influencing it through key signaling cascades, such as PI3K/AKT/mTOR and JAK/STAT[38–40]. In our study, hsa-miR-19a was significantly upregulated in PD-L1-positive BTC, consistent with previous reports in lung cancer cells[41]. Two miRNAs in our classifier, hsa-miR-93-5p and hsa-miR-16-5p, have been linked to immune regulation via PD-L1 modulation. miR-93-5p promotes tumor growth by targeting the PD-L1/CCND1 axis in breast cancer, while miR-16-5p suppresses PD-L1 expression and inhibits tumor progression in lung adenocarcinoma, highlighting their potential as biomarkers for PD-L1–based immunotherapy[42,43]. Upregulation of hsa-miR-126-3p may suppress the PI3K/AKT/mTOR signaling pathway and be involved in angiogenesis and vascular homeostasis, which can influence immune cell infiltration into the tumor[44,45]. These immunological associations support the biological relevance of our miRNA signature and suggest directions for future mechanistic studies in BTC.

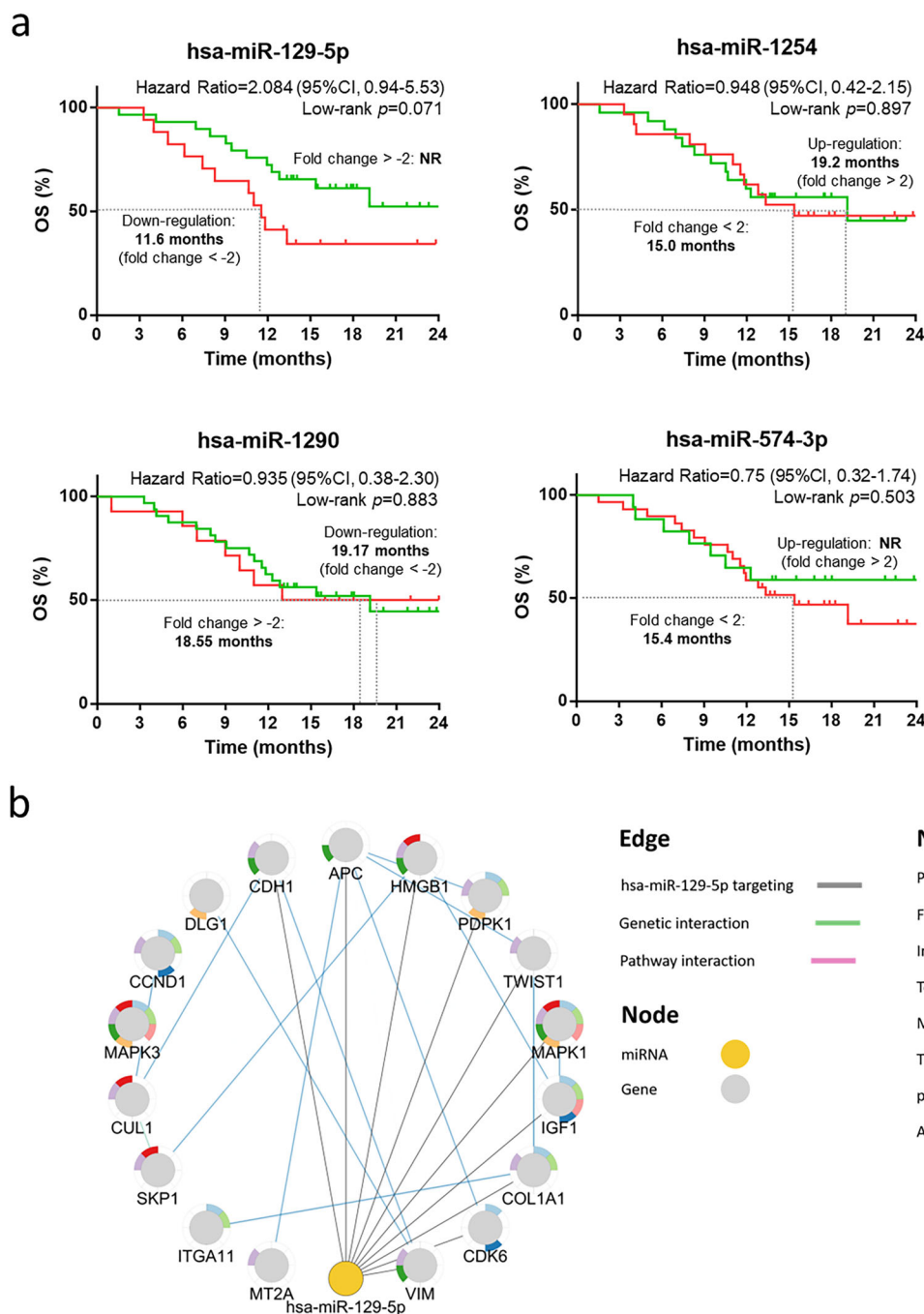The construction of an miRNA signature to predict BTC outcomes is not new[10–12]. However, previous studies typically enrolled heterogeneous patient populations across stages I–IV, limiting their applicability to patients with advanced BTC who received chemoimmunotherapy. In this study, we developed a 3-miRNA predictive model that was specifically tailored to this clinical context. To enhance its predictive utility, we integrated TMB, which resulted in a predictive accuracy of 0.92 for PFS. This composite biomarker may improve risk stratification and guide clinical decision-making in patients with advanced BTC receiving standard chemoimmunotherapy. Although MSI-H status has been previously reported as a biomarker associated with a higher TMB and a favorable outcome of immunotherapy in BTC, the prevalence of MSI-H in BTC is generally as low as 1.5% in TOPAZ-1 and 2.1% in our study[2,18,46]. Therefore, MSI-H was not incorporated into our prediction model. As all patients received the same treatment and the classifier correlated with both response and outcomes, our findings support a potentially predictive role for this classifier. Nonetheless, without a chemotherapy-only comparator, we could not exclude the possibility that the signature also reflects a broader disease biology. Further validation in various treatment settings is required to confirm its predictive specificity.

Given the multifactorial nature of the treatment response, we employed ML to capture the complex interactions between miRNAs and TMB. Despite the modest sample size, the model robustness was supported by cross-validation and AUC performance. With appropriate validation, ML remains applicable even to small biomedical datasets, offering a practical approach for integrative biomarker development in BTC[17].

Additionally, we assessed the levels of several miRNAs which are reported to be related to resistance to gemcitabine, cisplatin, or 5-FU, including hsa-miR-21, hsa-miR-200b, hsa-miR-210, hsa-miR-130a-3p, hsa-miR-199a-3p, and hsa-miR-106b[14,47–51]. In our study, no differences in treatment response, PFS, or OS were correlated with miRNA levels. All previous studies have established findings from certain chemotherapy-resistant BTC cell lines and validated them using relatively heterogeneous patient datasets. In contrast, our study population was homogeneous, with all patients receiving chemotherapy, which is the current standard treatment, rather than single-agent chemotherapy. Thus, our findings reliably illustrate the importance of miRNAs in the prognostic prediction of advanced BTC in clinical settings.

We also explored the dynamic changes in circulating miRNA expression before and after treatment. Although several miRNAs showed significant upregulation or downregulation in both responders and non-responders, these changes were not associated with differences in PFS or OS. In our results, hsa-miR-129-5p was significantly downregulated in non-responders. Prior studies have suggested that hsa-miR-129-5p could be induced by interferon beta, and knockdown of hsa-miR-129-5p may contribute to an immunosuppressive status with reduced expression of proinflammatory factors[52,53]. These findings highlight the potential biological relevance of dynamic miRNA alterations, which may reflect tumor evolution or immune modulation in response to therapy. While no circulating miRNAs have been validated for real-time disease monitoring in BTC, our results support further investigation of longitudinal miRNA profiling in future studies with larger cohorts and more frequent time points to identify novel biomarkers.

This study had some limitations. First, the relatively small sample size may have reduced the statistical power and increased the risk of overfitting in the ML model. Although cross-validation was used and an independent validation cohort was included, the limited number of patients in both cohorts may have affected the generalizability of our findings. The validation cohort also consisted of only seven patients treated with anti–PD-1 monotherapy, which differed from the combination regimen used in the discovery cohort and may have influenced the consistency of the results across treatment settings. Second, although the selected miRNAs were associated with both treatment response and outcomes, their initial selection was based on response in the discovery cohort, which may have contributed to a response-driven association with PFS and OS. Third, without a chemotherapy-only comparator arm, it was difficult to determine whether the predictive value of the miRNA signature was specific to immunotherapy or reflected the general treatment sensitivity. Finally, although clinical

**Fig. 4 | Dynamic change in hsa-miR-129-5p, hsa-miR-1254, hsa-miR-1290, and hsa-miR-574-3p between pre- and post-treatment plasma samples. a** Forty-six patients were divided into two groups based on the down-regulated expression of hsa-miR-129-5p or hsa-miR-1290, with a threshold of a twofold decrease. In contrast, the expression of hsa-miR-1254 and hsa-miR-574-3p was each divided into two groups based on a twofold increase. Only a borderline significant difference ($0.05 \le p \le 0.1$) in OS was observed in relation to the dynamic change in hsa-miR-129-5p. **b** Data from STRING-DB showed the pathways related to hsa-miR-129-5p and its target genes.

correlations between miRNA expression and treatment outcomes have been demonstrated, the underlying biological mechanisms have not been explored through in vitro or in vivo experiments. Further research is needed to elucidate the functional roles of these miRNAs in shaping the tumor-immune microenvironment. Despite these limitations, this study represents one of the first prospective investigations of blood-based biomarkers in chemoimmunotherapy-treated ABTC, highlighting the potential of circulating miRNAs in informing personalized treatment strategies.

In conclusion, our study highlighted the potential predictive role of miRNAs in advanced BTC and developed a novel 3-miRNA model to predict therapeutic response to chemoimmunotherapy, aiding clinicians in formulating treatment strategies.

## Methods
### Patient enrollment and sample collection
The T1219 trial was a single-arm, multicenter phase II study conducted in Taiwan. Patients with treatment-naïve, locally advanced, or metastatic BTC were enrolled and treated with a study regimen that included an intravenous infusion of a fixed dose of 240 mg nivolumab and 800 mg/m² gemcitabine on day 1, combined with oral administration of S-1 from days 1–10 in a

2-week cycle. Treatment was continued until disease progression, intolerable toxicity, withdrawal of consent, or any other reason.

The primary endpoint of the study was the objective response rate, defined using radiographic imaging studies according to the Response Evaluation Criteria in Solid Tumors, version 1.1. CR and PR were categorized as objective responses and were confirmed using two successive imaging studies. Secondary endpoints included PFS and OS. PFS was calculated as the time from the first dose to the first documented disease progression, death, or censoring date. OS was defined as the time from study entry to death or censorship of the study. The cutoff date for survival analysis was February 2023.

The trial protocol and post-hoc biomarker analyses were approved by the Institutional Review Board of Taipei Veterans General Hospital (2019–10-001 C), China Medical University Hospital (CMUH108-REC1–133) and National Cheng Kung University Hospital (A-BR-108–073), conducted in accordance with the Declaration of Helsinki and International Conference on Harmonization Good Clinical Practice guideline, and informed consent was obtained from all participants. This trial was registered at ClinicalTrials.gov (registration number: NCT04172402, date of registration 2019/11/18). One blood sample was collected from each patient at baseline before treatment, and a second sample was collected 6 weeks post-treatment (Fig. 1A). A 19–22 G needle was used to draw blood (5 mL) into a K2EDTA blood collection tube. Plasma was prepared from the blood sample using two centrifugation steps at room temperature. Briefly, the blood sample was centrifuged at $1200 \times g$ for 10 min, and the supernatant was centrifuged at $12,000 \times g$ for 10 min. The supernatant of the platelet-poor plasma was then transferred into a new 1.5 mL Eppendorf tube and stored at $-80\,°C$ until analysis. Before miRNA extraction, the risk of plasma sample hemolysis was assessed by measuring the absorbance at 414 and 375 nm using a DeNovix DS-11 spectrophotometer. Plasma samples were excluded from the study if the hemolysis ratio of A414 nm/A375 nm was >2.

### Plasma miRNA extraction and reverse transcription
The workflow of miRNA analysis is summarized in Fig. 1B. A total of 200 µL of plasma was used to extract plasma miRNA using the miRNeasy Serum/Plasma Advanced Kit (Cat. No. 217204, QIAGEN, Germany) and QIAcube Connect Fully Automated Nucleic Acid Extraction System (QIAGEN), according to the manufacturer's instructions. The resulting plasma miRNA was then eluted in 15 µL of nuclease-free water and stored at $-80\,°C$ until analysis. Prior to reverse transcription, plasma miRNA was quantified using the Qubit miRNA Assay Kit (Q32880, Thermo Fisher Scientific™, Waltham, MA, USA) with a Qubit 3.0 Fluorometer (Thermo Fisher) according to the manufacturer's protocol. A total of 2 ng of plasma miRNA was used for complementary DNA (cDNA) synthesis using the microRNA Universal RT Kit (Quark Biotechnology Taiwan, Inc.) according to the manufacturer's protocol. The 20 µL reaction mixture was then reverse transcribed using the following program: $42\,°C$ for 60 min, $95\,°C$ for 5 min, and $4\,°C$ indefinitely. The resulting cDNA was stored at $-80\,°C$ for later use.

### miRNA expression analysis
For miRNA expression profile analysis of each cDNA sample, 173 assays, including 167 miRNAs, two small nuclear RNAs (RNU6B and RNU43), three Spike-in Controls (Extraction Spike-in Control, RT Spike-in Control, and PanelChip Spike-in Control), and 18 s rRNAs, were performed simultaneously using the mirSCAN™ assay (Quark Biotechnology) on the NextAmp™ Analysis System (Quark Biotechnology). Biomarkers were selected for the mirSCAN™ assay based on their implications in cancer and their presence in human plasma[54]. cDNA samples from plasma miRNAs were used to perform the mirSCAN assay, according to the manufacturer's instructions. The mirSCAN™ program was set up as follows: $95\,°C$ for 3 min, 40 cycles at $95\,°C$ for 36 s, and $60\,°C$ for 72 s.

### Data processing and analysis
The miRNA expression profiles of the 46 patients included in the T1219 trial were normalized using the quantile normalization method[55]. For the

miRNA-based classifier analysis, miRNAs without amplification signals across 20% of each group were excluded from the analysis. Overall, 39 miRNAs were selected to develop an miRNA-based classifier based on the treatment responses of the patients (Table S1). These 46 patients were categorized into the training set. Features were standardized to zero mean and unit variance, and a Support Vector Machine (SVM) classifier with a radial basis function kernel was implemented using LIBSVM in the R package e1071 (version 1.6-8). The hyperparameters (cost and gamma) were optimized using a grid search combined with 10-fold cross-validation. The optimal parameters were cost = 45.3 and gamma = 0.00552, respectively. To mitigate overfitting, all parameter tuning was restricted to the training datasets. Seven additional patients with advanced BTC who were treated with anti-PD-1 were recruited from a different location as an independent real-world validation cohort.

### Statistical analysis
The types of gene-gene and miRNA target interactions were identified using STRING-DB v11.5[56] and visualized using Cytoscape 3.9. Dynamic changes in miRNA levels were compared with pre- and post-treatment miRNA profiles. Differentially expressed miRNAs were identified according to fold change $> \pm 1.5$ and $p < 0.05$. Survival analyses were performed using GraphPad Prism (v.6.01; GraphPad Inc.). Kaplan–Meier survival curves were generated to estimate OS and PFS, and the log-rank test was used to compare survival between the groups. Hazard ratios (HRs) and 95% CI were calculated using the Cox proportional hazards model. A two-sided $p < 0.05$ was considered statistically significant.

### Data Availability
The datasets generated and analyzed during the current study are not publicly available due to privacy or ethical restrictions but are available from the corresponding author on reasonable request.

### References
1. Chan, K.-M. et al. Characterization of intrahepatic cholangiocarcinoma after curative resection: outcome, prognostic factor, and recurrence. *BMC Gastroenterol.* **18**, 180 (2018).
2. Oh, D. Y. et al. Durvalumab plus gemcitabine and cisplatin in advanced biliary tract cancer. *NEJM Evid.* **1**, EVIDoa2200015 (2022).
3. Kelley, R. K. et al. Pembrolizumab in combination with gemcitabine and cisplatin compared with gemcitabine and cisplatin alone for patients with advanced biliary tract cancer (KEYNOTE-966): a randomised, double-blind, placebo-controlled, phase 3 trial. *Lancet* **401**, 1853–1865 (2023).
4. Yue, S., Zhang, Y. & Zhang, W. Recent advances in immunotherapy for advanced biliary tract cancer. *Curr. Treat. Options Oncol.* **25**, 1089–1111 (2024).
5. Chiang, N. et al. MO50-3 TCOG T3221 study: the registry of genetic alterations of Taiwan biliary tract cancer. *Ann. Oncol.* **35**, S1355 (2024).
6. Le, D. T. et al. Mismatch repair deficiency predicts response of solid tumors to PD-1 blockade. *Science* **357**, 409–413 (2017).
7. Macias, R. I. R. et al. Diagnostic and prognostic biomarkers in cholangiocarcinoma. *Liver Int.* **39**, 108–122 (2019).
8. Mody, K. et al. Circulating tumor DNA profiling of advanced biliary tract cancers. *JCO Precis Oncol.* **3**, 1–9 (2019).
9. Peng, Y. & Croce, C. M. The role of MicroRNAs in human cancer. *Signal Transduct. Target Ther.* **1**, 15004 (2016).
10. Wada, Y. et al. A blood-based noninvasive miRNA signature for predicting survival outcomes in patients with intrahepatic cholangiocarcinoma. *Br. J. Cancer* **126**, 1196–1204 (2022).
11. Zhang, M. Y. et al. Identification of a novel microRNA signature associated with intrahepatic cholangiocarcinoma (ICC) patient prognosis. *BMC Cancer* **15**, 64 (2015).

12. Barbato, A. et al. Micro-RNA in cholangiocarcinoma: implications for diagnosis, prognosis, and therapy. *J. Mol. Pathol.* **3**, 88–103 (2022).

13. Okamoto, K., Miyoshi, K. & Murawaki, Y. miR-29b, miR-205 and miR-221 enhance chemosensitivity to gemcitabine in HuH28 human cholangiocarcinoma cells. *PLoS One* **8**, e77623 (2013).

14. Jiao, D. et al. miR-106b regulates the 5-fluorouracil resistance by targeting Zbtb7a in cholangiocarcinoma. *Oncotarget* **8**, 52913–52922 (2017).

15. Omar, H. A. et al. Immunomodulatory microRNAs in cancer: targeting immune checkpoints and the tumor microenvironment. *FEBS J.* **286**, 3540–3557 (2019).

16. Teufel, M. et al. Circulating miRNA biomarkers predicting regorafenib (REG) clinical benefit in patients with hepatocellular carcinoma (HCC) in the resorce trial. *Ann. Oncol.* **28**, v240 (2017).

17. Rajakumar, T. et al. A blood-based miRNA signature with prognostic value for overall survival in advanced stage non-small cell lung cancer treated with immunotherapy. *NPJ Precis Oncol.* **6**, 19 (2022).

18. Chiang, N. J. et al. Impaired chromatin remodeling predicts better survival to modified gemcitabine and S-1 plus nivolumab in advanced biliary tract cancer: a phase II T1219 study. *Clin. Cancer Res.* **28**, 4248–4257 (2022).

19. Juarez, J. J., Osataphan, S. A., Ponvilawan, B., Charoenngam, N. & Peters, M. L. B. PD-L1 as a predictor of chemo-immunotherapy response in biliary tract cancers: a systematic review and meta-analysis. *JCO* **42**, 541–541 (2024).

20. Lou, Y., Chen, Y., Guo, K., Li, B. & Zheng, S. Emerging biomarkers for immunotherapy response in biliary tract cancers: a comprehensive review of immune checkpoint inhibitor strategies. *Biomark. Med.* **18**, 703–715 (2024).

21. Budczies, J. et al. Tumour mutational burden: clinical utility, challenges and emerging improvements. *Nat. Rev. Clin. Oncol.* **21**, 725–742 (2024).

22. Rodrigues, P. M. et al. Next-generation biomarkers for cholangiocarcinoma. *Cancers* **13**, 3222 (2021).

23. Zhang, N. et al. Liquid biopsy-based prediction of clinical benefit from immune checkpoint inhibitors in advanced biliary tract cancer. *JCO* **42**, e16179 (2024).

24. Hwang, S. et al. Concordance of ctDNA and tissue genomic profiling in advanced biliary tract cancer. *J Hepatol*. **82**, 649–657 (2024).

25. Dong, L. et al. The roles of MiRNAs (MicroRNAs) in melanoma immunotherapy. *Int J. Mol. Sci.* **23**, 14775 (2022).

26. Shi, T., Morishita, A., Kobara, H. & Masaki, T. The role of microRNAs in cholangiocarcinoma. *Int. J. Mol. Sci*. **22**, 167–180 (2021).

27. Msheik, Z. S. et al. miR-126 decreases proliferation and mammosphere formation of MCF-7 and predicts prognosis of ER+ breast cancer. *Diagnostics* **12**, 745 (2022).

28. Liu, B., Peng, X. C., Zheng, X. L., Wang, J. & Qin, Y. W. MiR-126 restoration down-regulate VEGF and inhibit the growth of lung cancer cell lines in vitro and in vivo. *Lung Cancer* **66**, 169–175 (2009).

29. Poleto Spinola, L. et al. Underexpression of miR-126-3p in patients with cholangiocarcinoma. *Asian Pac. J. Cancer Prev.* **22**, 573–579 (2021).

30. Jusufović, E. et al. let-7b and miR-126 are down-regulated in tumor tissue and correlate with microvessel density and survival outcomes in non-small-cell lung cancer. *PLoS One* **7**, e45577 (2012).

31. McNally, M. E. et al. Concomitant dysregulation of microRNAs miR-151-3p and miR-126 correlates with improved survival in resected cholangiocarcinoma. *HPB* **15**, 260–264 (2013).

32. Han, S. et al. Suppression of miR-16 promotes tumor growth and metastasis through reversely regulating YAP1 in human cholangiocarcinoma. *Oncotarget* **8**, 56635–56650 (2017).

33. Meijer, L. L. et al. Unravelling the diagnostic dilemma: a microRNA panel of circulating MiR-16 and MiR-877 as a diagnostic classifier for distal bile duct tumors. *Cancers* **11**, 1181 (2019).

34. Shi, X. et al. microRNA-93-5p promotes hepatocellular carcinoma progression via a microRNA-93-5p/MAP3K2/c-Jun positive feedback circuit. *Oncogene* **39**, 5768–5781 (2020).

35. Vila-Navarro, E. et al. MiR-93 is related to poor prognosis in pancreatic cancer and promotes tumor progression by targeting microtubule dynamics. *Oncogenesis* **9**, 43 (2020).

36. Liang, H. et al. miR-93 functions as an oncomiR for the downregulation of PDCD4 in gastric carcinoma. *Sci. Rep.* **6**, 23772 (2016).

37. Yuan, F. et al. Exosomal miR-93-5p as an important driver of bladder cancer progression. *Transl. Androl. Urol.* **12**, 286–299 (2023).

38. Lin, X. et al. Regulatory mechanisms of PD-1/PD-L1 in cancers. *Mol. Cancer* **23**, 108 (2024).

39. Danbaran, G. R. et al. How microRNAs affect the PD-L1 and its synthetic pathway in cancer. *Int Immunopharmacol.* **84**, 106594 (2020).

40. Cha, J. H., Chan, L. C., Li, C. W., Hsu, J. L. & Hung, M. C. Mechanisms controlling PD-L1 expression in cancer. *Mol. Cell.* **76**, 359–370 (2019).

41. Ma, Y. et al. Tumor-intrinsic PD-L1 exerts an oncogenic function through the activation of the Wnt/β-catenin pathway in human non-small cell lung cancer. *Int. J. Mol. Sci.* **23**, 11031 (2022).

42. Yang, M. et al. MiR-93-5p regulates tumorigenesis and tumor immunity by targeting PD-L1/CCND1 in breast cancer. *Ann. Transl. Med.* **10**, 203 (2022).

43. Chen, H. L. et al. Serum exosomal miR-16-5p functions as a tumor inhibitor and a new biomarker for PD-L1 inhibitor-dependent immunotherapy in lung adenocarcinoma by regulating PD-L1 expression. *Cancer Med.* **11**, 2627–2643 (2022).

44. Wang, S. et al. The endothelial-specific microRNA miR-126 governs vascular integrity and angiogenesis. *Dev. Cell.* **15**, 261–271 (2008).

45. Chen, Q., Chen, S., Zhao, J., Zhou, Y. & Xu, L. MicroRNA-126: a new and promising player in lung cancer. *Oncol. Lett.* **21**, 35 (2021).

46. Yang, X. et al. Genomic characterization and immunotherapy for microsatellite instability-high in cholangiocarcinoma. *BMC Med.* **22**, 42 (2024).

47. Asukai, K. et al. Micro-RNA-130a-3p regulates gemcitabine resistance via pparg in cholangiocarcinoma. *Ann. Surg. Oncol.* **24**, 2344–2352 (2017).

48. Silakit, R. et al. Potential role of HIF-1-responsive microRNA210/HIF3 axis on gemcitabine resistance in cholangiocarcinoma cells. *PLoS One* **13**, e0199827 (2018).

49. Wu, Z., Jiang, S. & Chen, Y. Non-coding RNA and drug resistance in cholangiocarcinoma. *Noncoding RNA Res.* **9**, 194–202 (2024).

50. Li, Q. et al. MiR-199a-3p enhances cisplatin sensitivity of cholangiocarcinoma cells by inhibiting mTOR signaling pathway and expression of MDR1. *Oncotarget* **8**, 33621–33630 (2017).

51. Meng, F. et al. Involvement of human micro-RNA in growth and response to chemotherapy in human cholangiocarcinoma cell lines. *Gastroenterology* **130**, 2113–2129 (2006).

52. Zhang, J. et al. Interferon-β induced microRNA-129-5p down-regulates HPV-18 E6 and E7 viral gene expression by targeting SP1 in cervical cancer cells. *PLoS One* **8**, e81366 (2013).

53. Zhang, H. Y. et al. miR-129-5p regulates the immunomodulatory functions of adipose-derived stem cells via targeting stat1 signaling. *Stem Cells Int.* **2019**, 2631024 (2019).

54. Hsieh, C.-H. et al. A novel multi-gene detection platform for the analysis of miRNA expression. *Sci. Rep.* **8**, 10684 (2018).

55. Bolstad, B. M., Irizarry, R. A., Astrand, M. & Speed, T. P. A comparison of normalization methods for high density oligonucleotide array data based on variance and bias. *Bioinformatics* **19**, 185–193 (2003).

56. Szklarczyk, D. et al. STRING v11: protein-protein association networks with increased coverage, supporting functional discovery in genome-wide experimental datasets. *Nucleic Acids Res.* **47**, D607–d613 (2019).

## Author contributions

All authors contributed to the study's conception and design. N.J.C: investigation, formal analysis, funding acquisition, project administration, and draft writing. C.Y.T: formal analysis, draft writing. L.Y.B: investigation and project administration. P.C.C: data curation, formal analysis and draft writing. W.M.C: data curation, formal analysis and draft writing. S.T.K: data curation, formal analysis and draft writing. S.C.C: investigation and draft reviewing. M.H.C: investigation, supervision, and draft reviewing. C.H.H: investigation, data curation, formal analysis, resources, and draft reviewing.

## Competing interests

Authors PCC, WMC, and STK are employees of Quark Biotechnology, Inc. All other authors declare no financial or nonfinancial competing interests.

## Additional information

**Supplementary information** The online version contains supplementary material available at https://doi.org/10.1038/s41698-025-01099-x.

**Correspondence** and requests for materials should be addressed to Jason Chia-Hsun Hsieh.

**Reprints and permissions information** is available at http://www.nature.com/reprints

**Publisher's note** Springer Nature remains neutral with regard to jurisdictional claims in published maps and institutional affiliations.